Global response of the terrestrial biosphere to CO_2 and climate change using a coupled climate-carbon cycle model

M. Berthelot, P. Friedlingstein, P. Ciais, and P. Monfray

Institut Pierre-Simon Laplace, Laboratoire des Sciences du Climat et de l'Environnement, Commissariat à l'Energie Atomique-Saclay, Gif sur Yvette, France

J. L. Dufresne, H. Le Treut, and L. Fairhead

Institut Pierre-Simon Laplace, Laboratoire de Météorologie Dynamique, Université Pierre et Marie Curie, Paris, France

[1]   We study the response of the land biosphere to climate change by coupling a climate general circulation model to a global carbon cycle model. This coupled model was forced by observed CO_2 emissions for the 1860–1990 period and by the IPCC SRES-A2 emission scenario for the 1991–2100 period. During the historical period, our simulated Net Primary Production (NPP) and net land uptake (NEP) are comparable to the observations in term of trend and variability. By the end of the 21st century, we show that the global NEP is reduced by 56% due to the climate change. In the tropics, increasing temperature, through an increase of evapotranspiration, acts to reduce the soil water content, which leads to a 80% reduction of net land CO_2 uptake. As a consequence, tropical carbon storage saturates by the end of the simulation, some regions becoming sources of CO_2. On the contrary, in northern high latitudes, increasing temperature stimulates the land biosphere by lengthening the growing season by about 18 days by 2100 which in turn leads to a NEP increase of 11%. Overall, the negative climate impact in the tropics is much larger than the positive impact simulated in the extratropics, therefore, climate change reduce the global land carbon uptake. This constitutes a positive feedback in the climate-carbon cycle system.   *INDEX TERMS:* 0315 Atmospheric Composition and Structure: Biosphere/atmosphere interactions; 1615 Global Change: Biogeochemical processes (4805); 1630 Global Change: Impact phenomena; *KEYWORDS:* climate change impact, terrestrial carbon cycle

1.   Introduction

[2]   As a result of human activities (fossil fuels combustion and land use change), the atmospheric concentration of carbon dioxide has increased by about 30% since 1860 (Figure 1). The induced positive radiative forcing tends to warm the surface. Indeed, the global temperature has risen up by $0.6°C$ over the same period. This increase of temperature is modulated by other greenhouse gases and aerosols changes, but it is most likely that if the atmospheric CO_2 continue to increase, a larger climate change would occur in the future [*Intergovernmental Panel on Climate Change (IPCC)*, 2001].

[3]   Over the last decade, the annual increase of atmospheric carbon reached 2.9 ± 0.1 Gt C yr^{-1} [*IPCC*, 2001]. This rate of increase is less than half of the estimated anthropogenic CO_2 emissions (fossil fuels = 6.3 ± 0.4 Gt C yr^{-1} and deforestation = 1.6 ± 0.8 Gt C yr^{-1} during the 1990–1998

period, [*IPCC*, 2001]), the other part being absorbed by the oceans and by the terrestrial biosphere. Land and ocean carbon cycles are, among other things, controlled by climate and atmospheric CO_2. There is therefore an intimate coupling between climate change and the global carbon cycle and it is thus very important to characterize and quantify this coupling in the context of future climate prediction.

[4]   The way both carbon cycle and climate system will interact in the future are however sources of a lot of uncertainties, namely, the climate sensitivity to greenhouse gases (GHG) and aerosols [*Cubasch and Fisher-Bruns*, 2000; *Meehl et al.*, 2000], the global carbon cycle and its response to climate change [*Cramer et al.*, 2001] and the economical uncertainty due to the GHG emissions scenarios [*Nakicenovic et al.*, 2000]. Several modeling studies estimate the impact of increasing atmospheric CO_2 and future climate change on the terrestrial carbon cycle. To do so, they usually force their terrestrial model with future climates computed by a Global Circulation Model (GCM) forced either by a prescribed transient increase of atmospheric CO_2 [*Cao and Woodward*, 1998; *Cramer et al.*, 2001; *Friedlingstein et al.*,
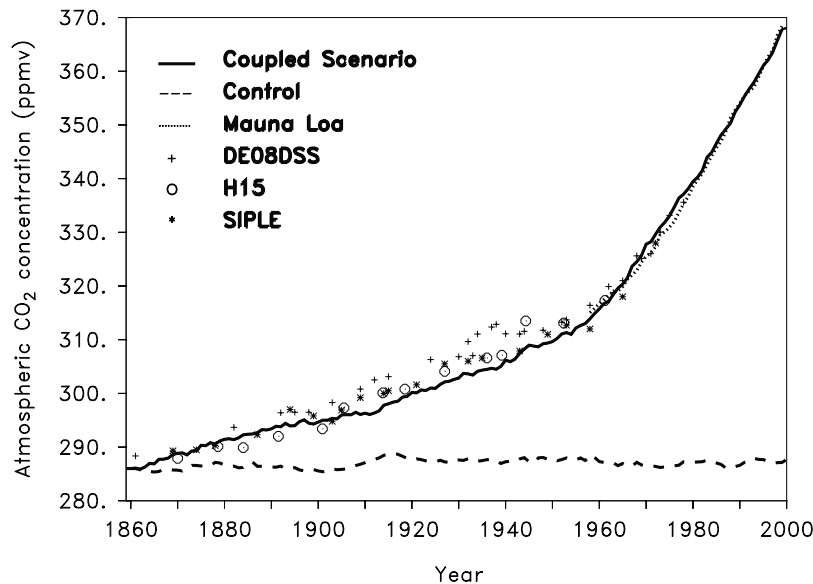
Figure 1. Time series of the atmospheric CO_2 concentrations simulated by the climate-carbon cycle coupled model for the Control run (dashed line) and the Coupled Scenario run (solid line). Also shown, in symbols, the observed atmospheric CO_2 from three Antarctic ice cores (DE08 and DSS [*Etheridge et al.*, 1996], H15 [*Kawamura et al.*, 1997], Siple [*Friedli et al.*, 1986]) and from Mauna Loa measurements [*Keeling et al.*, 1995].

2001] or by a doubling of the CO_2 concentration [*Betts et al.*, 1997; *King et al.*, 1997; *Melillo et al.*, 1993; *Neilson and Drapek*, 1998]. The main outcome of these studies is that the terrestrial biosphere is strongly affected by the climate change. Therefore, future atmospheric CO_2 will be driven not only by the emission scenario, but also by the efficiency of land and ocean to absorb CO_2 under the future climate. Hence, a consistent estimate of future atmospheric CO_2 and future climate requires a fully coupled climate-carbon model. In a recent study using a GCM coupled to carbon cycle models, *Cox et al.* [2000] found that the global warming will be amplified because of the positive feedback between terrestrial carbon cycle and the climate change. An important point highlighted by *Cox et al.* [2000] is that the land biosphere will become a large source of carbon to the atmosphere after 2050 induced by the dieback of Amazonian rain forests and by a global increase of soil carbon respiration.

[5] Here, we use the IPSL fully coupled climate-carbon cycle simulation [*Dufresne et al.*, 2002] to analyze in details the impact of future climate change on the terrestrial carbon cycle. We first describe the models used and the simulations performed. Then, we evaluate the model performance against the historical period. Finally, we quantify the response of the terrestrial biosphere to rising CO_2 and changing climate over the 21st century. To do so, we perform additional simulations in order to identify which climate variables control the simulated response.

2. Models and Coupling Description
2.1. Description of the Climate and Ocean Carbon Models

[6] The climate model used is a 3-dimensional coupled Ocean-Atmosphere General Circulation Model (OAGCM),

composed of an ocean circulation model (OPA-ICE [*Delecluse et al.*, 1993]) and a atmospheric model (LMD-5.3 [*LeTreut and Li*, 1991]). A coupler (OASIS [*Terray et al.*, 1995]) is used to ensure spatial interpolation and time synchronization when exchanging variables between the atmosphere and the ocean.

[7] The oceanic carbon cycle model, HAMOCC3 [*Maier-Reimer*, 1993] computes ocean biological carbon fluxes based on dissolved phosphates, and links marine export production to phosphate utilization. It has been adapted to OPA-ICE OGCM [*Aumont*, 1998] and is forced by monthly mean fields of ocean circulation, temperature, salinity, wind, sea ice and fresh water fluxes at surface.

2.2. Description of the Terrestrial Biosphere Model

[8] The terrestrial carbon cycle model, SLAVE [*Friedlingstein et al.*, 1995], runs at the same horizontal spatial resolution than the Atmospheric GCM. It accounts for nine natural ecosystems and croplands [*Friedlingstein et al.*, 1995]. In SLAVE, terrestrial carbon cycling is driven by the GCM monthly fields of surface temperature, precipitation, solar radiation and by the annual atmospheric CO_2 concentration which directly influences Net Primary Productivity (NPP). The model computes the water budget, net primary productivity, allocation, phenology, biomass, litter and soil carbon budgets. Carbon assimilated through NPP is allocated to three phytomass pools: leaves, stems and roots. Litter and soil carbon pools are both divided into metabolic and structural components. NPP is computed by SLAVE as a function of the three climatic variables following an ε formulation of NPP as developed in the CASA model [*Potter et al.*, 1993]. NPP is proportional to absorbed photosynthetically active radiation

(APAR) and is scaled down by temperature and precipitation stress factors.

$$NPP_0 = \varepsilon \times APAR \times T_{\varepsilon 1} \times T_{\varepsilon 2} \times W_\varepsilon \qquad (1)$$

APAR is deduced from incoming solar radiation and from Leaf Area Index (LAI) [Sellers et al., 1996], LAI being diagnosed from the calculated leaf biomass. ε is the maximum light use efficiency. The two temperature stress factors, $T_{\varepsilon 1}$ and $T_{\varepsilon 2}$, depress NPP at very high and low temperature and when the temperature is above or below the optimum temperature [Potter et al., 1993]. Note that we assume here that the optimum temperature for photosynthesis does not change in the future as we use a fixed vegetation map. The precipitation stress term, W_ε, is function of evapotranspiration and varies from 0 in very dry ecosystems to 1 in very wet ecosystems.

[9] The soil water content Q_m is function of monthly precipitation (PPT_m), of potential evapotranspiration (PET_m), which is calculated following Thornthwaite formulation [Thornthwaite, 1948; Thornthwaite and Mather, 1957], and of runoff (RUN_m). If monthly precipitation is larger than monthly evapotranspiration, the surface water content is increased by the difference between precipitation and evapotranspiration and the excess water runs off. On the contrary, if precipitation are insufficient to satisfy plant request, the plant uses the totality of precipitation and a fraction of soil water content.

[10] The fertilization effect, increase of NPP in response to increasing CO_2 [DeLucia et al., 1999; Wullschleger et al., 1995], is modeled as a β factor formulation [Friedlingstein et al., 1995].

[11] For each of the four litter and soil pools, heterotrophic respiration (RH) is calculated as the product of the pool carbon content by a pool specific decomposition rate (equation (2)). This rate depends on soil moisture and temperature (equation (3)) reflecting the fact that decomposition is favored by an increase of temperature or soil humidity.

$$RH = \sum_{i=1}^{4} K_i \times C_i \qquad (2)$$

where

$$K_i = K_{i, max} \times f_T \times f_{H2O} \qquad (3)$$

C_i represents the amount of carbon in soil and in litter pools. $K_{i,max}$, the optimal decomposition rate depends on the pool : litter K_{max} is equal to 10.4 yr^{-1} for metabolic fraction and 0.58 yr^{-1} for structural fraction and soil K_{max} is equal to 0.006 yr^{-1}. f_T is a Q_{10} function : a temperature increase of 10°C induces an increase of a factor of Q_{10} of the decomposition rate, with Q_{10} being fixed to 2 for each pool. The water function, f_{H2O}, first increases when soil water content increases. Above a threshold, it decreases to account for reduced decomposition under anaerobic conditions [Parton et al., 1993]. Finally, the net CO_2 flux between the land biosphere and the atmosphere, called the Net Ecosystem Production (NEP), is simply computed as the difference between NPP and RH.

[12] SLAVE suffers from three major limitations in this study. First, it does not account for land use changes such as deforestation or forest regrowth. Croplands are fixed at their present-day distribution based on the map of Matthews [1983]. Second, it does not take into account of natural vegetation dynamic. As for croplands, we use the present-day vegetation distribution [Matthews, 1983] across the entire simulation. Third, anthropogenic nitrogen deposition on land, a process which is believed to play a role in the present carbon balance, is not included in the model.

[13] We know these limitations may be of importance, however, the role of land cover changes and nitrogen deposition in the current carbon budget are still highly uncertain [Caspersen et al., 2000; Holland et al., 1997; Joos et al., 2002; Nadelhoffer et al., 1999; Pacala et al., 2001; Schimel et al., 2001]. Moreover, future changes in land cover may very likely to be mainly driven by the direct human activity rather than by climate change. In this pioneer study, where our main focus is the future response of the biosphere, we decided not to include these processes and to concentrate on the two major impacts of rising CO_2 and climate change.

2.3. Description of the Carbon-Climate Simulations

[14] Coupling between the carbon cycle models and the climate model is asynchronous, with a coupling time step of 1 year. The oceanic and terrestrial carbon models are driven by monthly climatic fields simulated by the OAGCM which itself is forced by annual atmospheric CO_2 concentration calculated the year before by the carbon models following equation (4).

$$CO_2^{i+1} = CO_2^i + (EMI^i - BIO^i - OCE^i)/2.12 \qquad (4)$$

where EMI^i, BIO^i and OCE^i represent the anthropogenic emissions, land biospheric and oceanic uptakes of CO_2 (in Gt C yr^{-1}) and CO_2^i is the CO_2 atmospheric concentration (in ppmv) of year i. The next year concentration CO_2^{i+1} is given to the OAGCM to simulate the next climate year. CO_2 is initialized at 286 ppmv for year 1860.

[15] Two 241-year long (from 1860 to 2100) coupled simulations were carried out (Table 1). The first simulation is a control simulation where anthropogenic CO_2 emissions are set to zero. Equation (4) becomes then $CO_2^{i+1} = CO_2^i - (BIO^i + OCE^i)/2.12$, that is atmospheric CO_2 concentration is only a function of uptake or release of carbon by land biosphere and ocean. The Control simulation is performed to assess the stability of the coupling, the absence of drift and to quantify the impact of internal climate variability on carbon fluxes. The second simulation, called Coupled Scenario run, uses prescribed anthropogenic CO_2 emissions following historical data before 1990 [Andres et al., 1996] and the IPCC/SRES-A2 emission scenario from 1990 up to 2100 [Nakicenovic et al., 2000]. Note that SRES-A2 emissions account for both fossil fuel emissions and deforestation fluxes. In the Coupled Scenario simulation, land and ocean carbon cycles respond to the atmospheric CO_2 increase and to the consequent climate change.

[16] In order to analyze the feedback between climate and carbon cycle, we perform two others simulations, the Fertilization and the Climate Impact simulations (Table 1). In the fertilization run, we use the same IPCC emission scenario, but we suppress the influence of the climate

Table 1. Simulations Description

Run Name	CO_2 Concentration	Climate
Control run	computed (no emissions)	computed
Coupled Scenario run	computed (A2-SRES scenario)	computed
Fertilization run	computed (A2-SRES scenario)	taken from the Control run
Climate Impact run	taken from the Fertilization run	taken from the Coupled Scenario run
Temperature Impact run	taken from the Fertilization run	taken from the Control run, except temperature taken from Coupled Scenario run
Precipitation Impact run	taken from the Fertilization run	taken from the Control run, except precipitation taken from Coupled Scenario run
Radiation Impact run	taken from the Fertilization run	taken from the Control run, except radiation taken from Coupled Scenario run
Soil Water Content Impact run	taken from the Fertilization run	taken from the Control run, except soil water content taken from Coupled Scenario run

change on the carbon cycle. That is to say, OCE^i and BIO^i are calculated using the climate of the Control simulation. The difference between this simulation and the Control one isolates the impact of CO_2 increase only on land.

[17] The difference in simulated uptakes between the Coupled Scenario run and the Fertilization run are primarily due to climate change (which tends to reduce the uptakes) but also, as a direct consequence, to higher atmospheric CO_2 (which tends to enhance the uptakes). The Climate Impact run uses the climate of the Coupled Scenario simulation and the atmospheric CO_2 of the Fertilization simulation. This last simulation allows us to separate the climate impact from the impact of additional atmospheric CO_2 on the carbon fluxes (Table 1). This simulation should be seen as the worst case scenario as the carbon fluxes are negatively impacted by the climate change but are not positively impacted by this additional atmospheric CO_2.

[18] In our modeling framework, the ocean and land carbon cycle responses are intimately coupled. For instance, if the land biosphere releases CO_2 to the atmosphere, then the ocean uptake will be stronger. In the following, we analyze only the response of the land biosphere, but it should be kept in mind that this response implicitly and indirectly is function of the role of the ocean. A symmetrical analysis of the ocean carbon cycle in the coupled carbon cycle-climate model is presented by *Bopp et al.* [2001].

3. Control Simulation and Evaluation of the Coupled Scenario Simulation Over the Historical Period

[19] The results from the Control simulation does not show any significant drift over the duration of the simulation (1860–2100). The variability of the calculated atmospheric concentration of CO_2 is about 3 ppmv around the initial value of 286 ppmv and does not show any trend larger than 1 ppmv per century (Figure 2). The simulated net terrestrial biospheric flux varies between -2.1 Gt C yr^{-1} and $+2.3$ Gt C yr^{-1}, with a mean value close to 0 Gt C yr^{-1} (Figure 3). Simulated NPP amounts to 57.5 ± 2.5 Gt C yr^{-1}. Carbon contents of phytomass, litter and soil are 547 ± 3 Gt C, 103 ± 1 Gt C and 1165 ± 4 Gt C, respectively.

[20] To evaluate the results of the Coupled Scenario simulation, we used data set available along the historical period (1860–1999). We compare the simulated atmospheric CO_2 concentration over the historical period to Antarctic ice

core measurements (DE08 and DSS [*Etheridge et al.*, 1996], H15 [*Kawamura et al.*, 1997], Siple [*Friedli et al.*, 1986]) combined with Mauna Loa measurements [*Keeling et al.*, 1995] as shown in Figure 1. The simulation compares well with observations, however, we underestimate atmospheric CO_2 during the period 1900–1940 [*IPCC*, 2001]. After 1960, the simulated CO_2 concentration matches well the atmospheric observations from Mauna Loa with a maximum difference of less than 1 ppmv. The simulated atmospheric CO_2 depends on the CO_2 emissions but also on the oceanic and land carbon uptakes. These latter are also simulated in a realistic amount. Indeed, the net land biospheric uptake reaches 1.9 Gt C yr^{-1} for the 1980s with a interannual variability of about 2.0 Gt C yr^{-1} over the 1980s. We simulate a NPP of 64 Gt C yr^{-1} in 2000 (Figure 3). These values are in the range of the recent estimations [*IPCC*, 2001; *Keeling et al.*, 1996; *Saugier and Roy*, 2001].

[21] In the Northern Hemisphere, the amplitude of the seasonal cycle of atmospheric CO_2, which is mainly driven by the seasonality of NEP, has increased by 22% at Mauna Loa (20°N) since 1960 [*Keeling et al.*, 1996]. We compared the amplitude change of atmospheric CO_2 at Mauna Loa with the amplitude change of the NEP of the Coupled Scenario simulation between 20°N and 90°N (Figure 4). The simulated NEP amplitude change reaches 12%, which is lower than the observations.

[22] Moreover, the simulated beginning of the growing season is advanced by 6 days in early April between 20°N and 90°N over the 1958–1990 period consistent with what is observed on atmospheric CO_2 in middle and high northern latitudes [*Keeling et al.*, 1996; *Keyser et al.*, 2000; *Menzel and Fabian*, 1999; *Myneni et al.*, 1997]. This advance is induced by temperature in our simulation, which increase by 0.5°C in Northern Hemisphere in March and April, in agreement with what is suggested by the observations [*Keyser et al.*, 2000; *Menzel and Fabian*, 1999; *Randerson et al.*, 1999].

[23] In summary, the Coupled Scenario simulation shows trends and variability in the carbon cycle that are consistent with the observations. However, in this study, NPP and hence NEP changes are entirely due to fertilization induced by increasing atmospheric CO_2 and to climate change. As mentioned before, we do not account for anthropogenic nitrogen deposition [*Bergh et al.*, 1999; *Bryant et al.*, 1998; *Holland et al.*, 1997; *Nadelhoffer et al.*, 1999; *Townsend et al.*, 1996] or land cover change such as forest
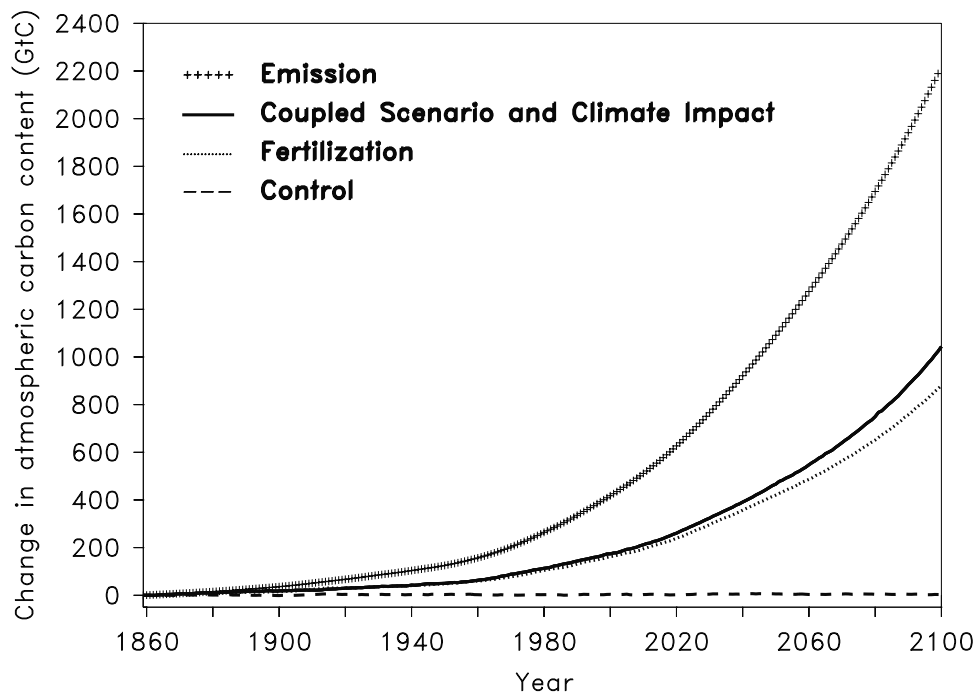
Figure 2. Time series of IPCC/SRES-A2 anthropogenic carbon emissions [*Nakicenovic et al.*, 2000] used as a forcing for the climate model (crosses) and simulated atmospheric carbon content change (departures from preindustrial Holocene) for the Control simulation (dashed line), the Coupled Scenario simulation (solid line) and the Fertilization simulation (dotted line). All numbers are in Gt C.
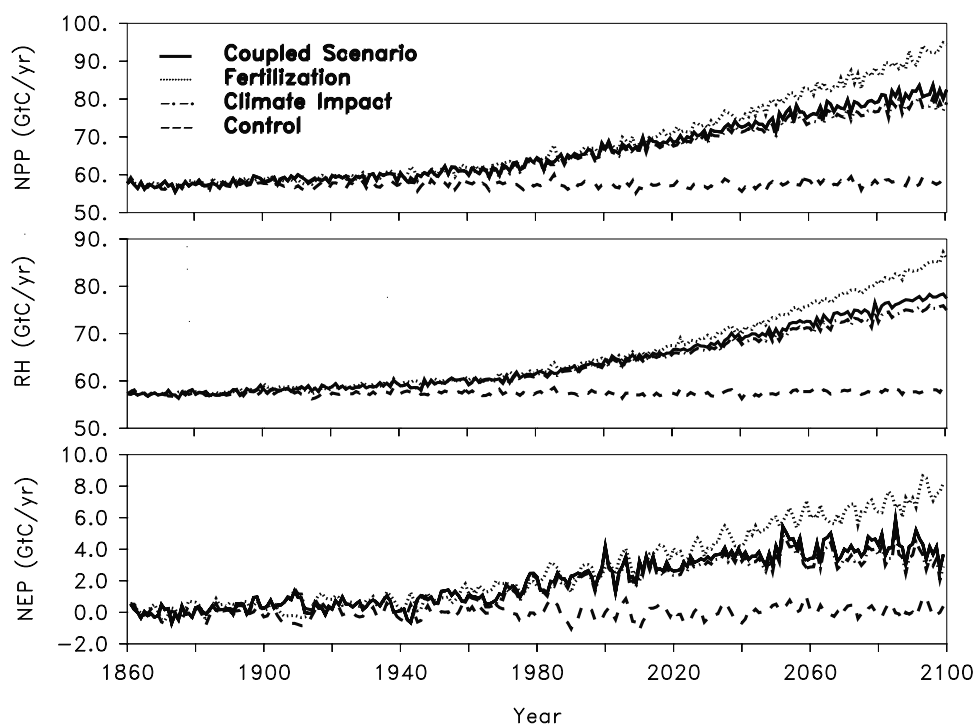
Figure 3. Time series of net primary production (NPP), heterotrophic respiration (RH), and net land carbon uptake (NEP) (in Gt C yr^{-1}) for the Control simulation (dashed line), the Coupled Scenario simulation (solid line), the Fertilization simulation (dotted line) and the Climate Impact simulation (dash-dotted line).
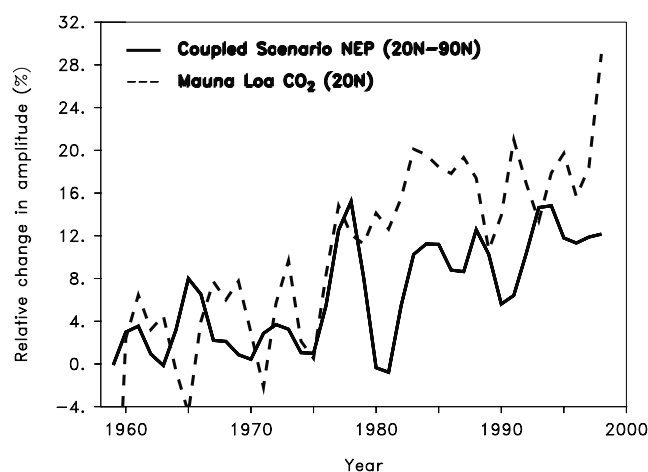
Figure 4. Time series of the relative evolution (in percent) of the seasonal amplitude of atmospheric CO_2 at Mauna Loa (20°N, dashed line) [*Keeling et al.*, 1995] compared to that of the NEP simulated by the Coupled Scenario run between 20°N and 90°N (solid line).

regrowth [*Caspersen et al.*, 2000; *Joos et al.*, 2002; *Pacala et al.*, 2001; *Schimel et al.*, 2001] and the consequences these phenomena could have on carbon cycling. Previous analyses has shown that impact on carbon cycle of atmospheric CO_2 increase, climate change, anthropogenic nitrogen deposition and croplands establishment and abandonment are not easily separable [*Friedlingstein et al.*, 1995; *Lloyd*, 1999; *McGuire et al.*, 2001] but they could all contribute to the net current biospheric sink [*Caspersen et al.*, 2000; *Joos et al.*, 2002; *Pacala et al.*, 2001; *Schimel et al.*, 2001]. The lower simulated than observed change of CO_2 amplitude could be due to the fact that we neglect land use changes and practice such as fertilizers utilization for crops [*McGuire et al.*, 2001; *Zimov et al.*, 1999]. As we are, at this present time, not able to separate the importance of these concurrent effects, this study should be taken as a preliminary step of coupled climate-carbon simulation considering an extreme formulation of factors influencing terrestrial carbon sink.

4. Land Responses Under Atmospheric Increasing CO_2 Only

[24] In this section, we analyze results from the Fertilization simulation where atmospheric CO_2 depends on IPCC emissions and oceanic and land CO_2 uptakes, these latter

being calculated with the Control climate (Table 1). By 2100, cumulated fossil fuel and land use emissions reach 2190 Gt C, only 980 Gt C remains in atmosphere (Figure 2), the rest (1310 Gt C) being absorbed by the ocean and by the land biosphere. Compared to 1860, terrestrial carbon increases by 640 Gt C by the end of the simulation (Table 2). More than half of this excess carbon (57%) is stored in the phytomass. One third accumulates in soils, the rest being stored in litter (Table 2). Sizewise, phytomass and litter pools increase by 65% by 2100 while soil carbon increases only by 18%. Within the living phytomass, as can be expected, most of carbon accumulates in wood. However, the rate of increase of excess carbon starts to decrease in wood around 2010, whereas it still increases in soils by 2100. It means that phytomass carbon begins to saturate, as opposed to soil carbon which has a long turnover time and accumulates an excess carbon over longer timescales.

[25] Regionally, two thirds of the carbon storage (416 Gt C in 2100) occurs in the tropics and southern extratropics (90°S–30°N) lands (Table 2). The last third is essentially stored in Northern Hemisphere deciduous and coniferous forests.

5. Terrestrial Responses Under Increasing CO_2 and Climate Change

[26] In the Coupled Scenario simulation, the overall effect of climate change (climate change alone + additional atmospheric CO_2) is to reduce terrestrial carbon uptake, the oceanic uptake being almost unchanged [*Dufresne et al.*, 2002].

[27] The cumulated land uptake reaches 465 Gt C by 2100, compared to 640 Gt C in the Fertilization run (Table 2). As a result, atmospheric CO_2 reaches 778 ppmv in 2100 in the Coupled Scenario run, compared to 700 ppmv in the Fertilization simulation (Figure 2). This positive climate feedback on atmospheric CO_2 is analyzed in detail by *Dufresne et al.* [2002]. Here we concentrate on analyzing the different mechanisms responsible for the global reduction of land uptake.

5.1. Global and Regional Responses

[28] The NPP simulated by the Coupled Scenario run reaches 82 Gt C yr^{-1} by 2100, compared to 94 Gt C yr^{-1} in the Fertilization run. This reduction of 12 Gt C yr^{-1} is the result of two opposite effects: (1) a reduction of NPP due to the climate change (Figure 5a), and (2) an increase of NPP due to the additional atmospheric CO_2. As mentioned in section 2.3., we use the Climate Impact simulation to

Table 2. Global Carbon Fluxes and Pools for the Control, the Coupled Scenario, the Fertilization, and the Climate Impact Runs[a]

	Control Run	Coupled Scenario Run	Fertilization Run	Climate Impact Run
NPP	58.3 (38.1/12.3/7.9)	81.5 (48.6/19.7/13.2)	94.2 (61.2/19.7/12.4)	78.4 (46.6/19.0/12.7)
RESP	58.3 (38.0/12.3/8.0)	77.9 (47.6/18.5/11.7)	85.5 (56.3/18.2/11.0)	75.5 (46.0/18.0/11.5)
NEP	0.0 (0.1/0.0/−0.1)	3.7 (1.0/1.2/1.5)	7.7 (4.9/1.4/1.4)	2.9 (0.6/1.0/1.2)
Terrestrial pools	1818 (1182/338/298)	2283 (1403/454/426)	2458 (1598/459/402)	2230 (1371/443/416)
Vegetation pool	551 (378/88/85)	850 (528/156/166)	915 (620/151/143)	818 (508/150/160)
Litter pool	104 (67/19/19)	139 (80/29/30)	167 (106/31/30)	134 (77/28/29)
Soil pool	1163 (737/232/194)	1294 (794/270/230)	1376 (871/276/228)	1278 (785/266/227)

[a]Values in parentheses are for the 90°S–30°N, 30°N–50°N and 50°N–90°N latitudinal bands, respectively. Fluxes are in Gt C yr^{-1} and pools are in Gt C.
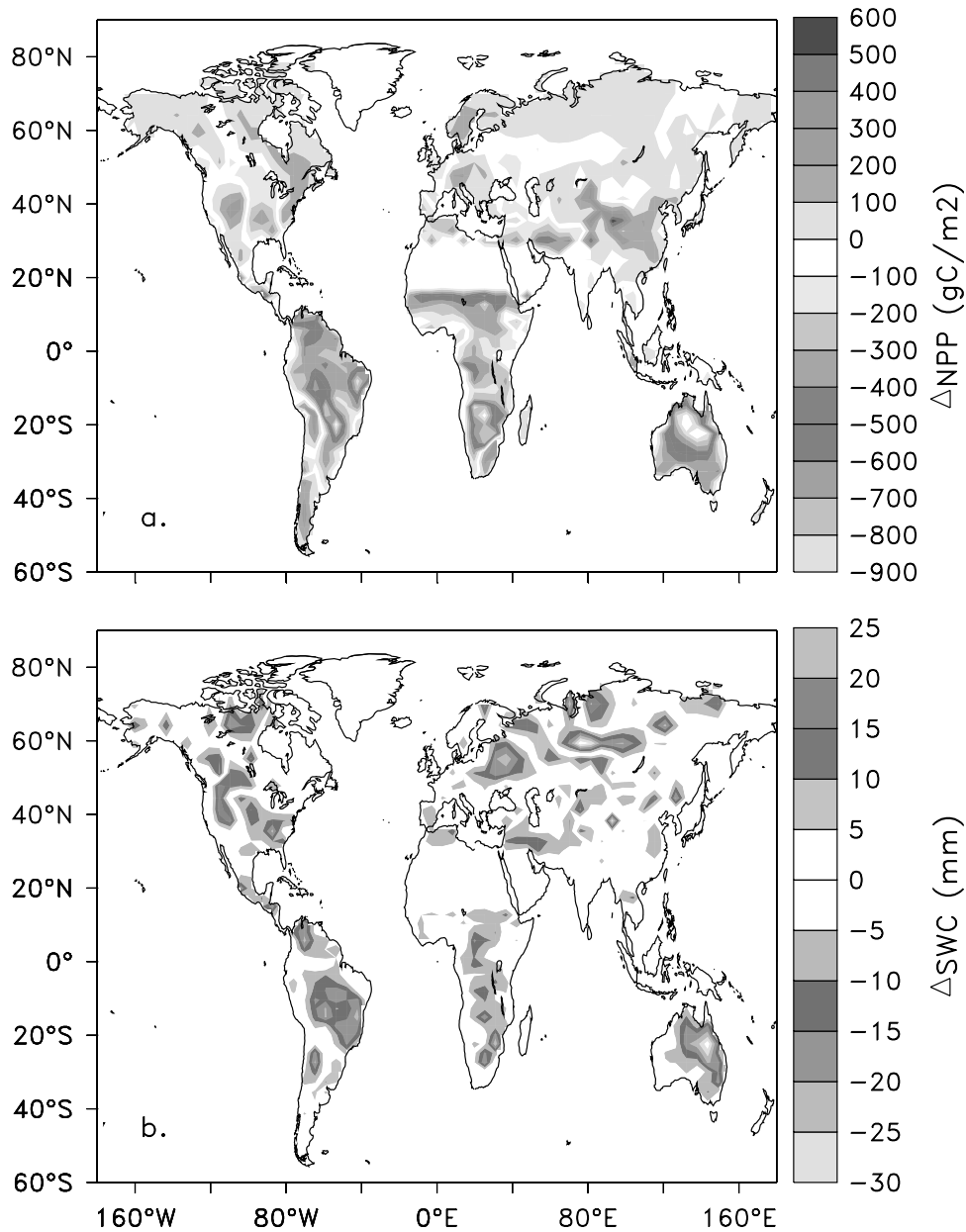
Figure 5. (a) Difference in NPP (in g C/m^2) between the Climate Impact simulation and the Fertilization simulation in 2100 (10-year average). Positive value means that NPP is increased under climate change only. (b) Difference in soil water content (in mm/yr) between the Climate Impact simulation and the Fertilization simulation in 2100 (10-year average). Positive value means that soil water content is increased under climate change. See color version of this figure at back of this issue.

separate these two effects. In this last run, NPP does not benefit from a higher atmospheric CO_2 and only reaches 78 Gt C yr^{-1} (Table 2).

[29] In the following we compare results from the Climate Impact and the Fertilization runs. As these two simulations are forced by the same atmospheric CO_2, they allow us to isolate the climate impact alone on the terrestrial biosphere.

[30] In the Climate Impact run, the increase of terrestrial carbon pool amounts to 412 Gt C by 2100 (to be compared with 640 Gt C in the Fertilization run, Table 2). Around 2100, NEP only amounts to 2.9 Gt C yr^{-1} in the Climate Impact run (to be compared with 7.7 Gt C yr^{-1} in the

Fertilization run) (Figure 3). Actually, by 2060, the NEP saturates around 4 Gt C yr^{-1} and begins to decrease after 2090, whereas NEP simulated by the Fertilization run continues to increase in 2100. Most of this climate impact occurs in the tropics, where NEP only reaches 0.6 Gt C yr^{-1} in the Climate Impact run, whereas it reaches 4.9 Gt C yr^{-1} in the Fertilization run by 2100 (Table 2). In the Northern Hemisphere middle and high latitudes (30°N–90°N), the impact of climate change is not so strong. Tundra and conifer forests show a small increase in NEP in response to climate change, while deciduous forests, grasslands and croplands shows the opposite.
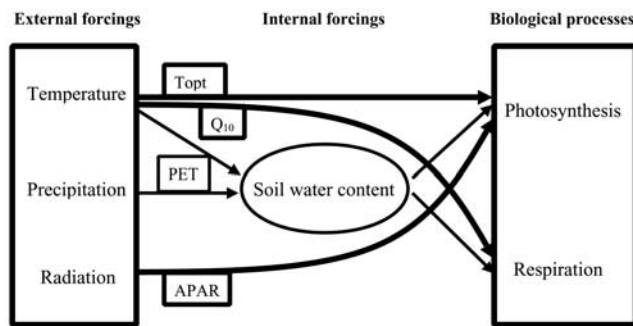
Figure 6. Conceptual scheme of the influences of temperature, precipitation, radiation and soil water content on land biosphere. NPP is directly influenced by temperature (solid arrow): it is depressed when temperature is below or above the optimum temperature (Topt). NPP is also directly influenced by solar radiation via the absorbed photosynthetically active radiation (APAR). Respiration directly increases with temperature as a Q_{10} function. NPP and RH are indirectly affected by temperature (through evapotranspiration, PET) and precipitation via the soil water content.

[31] Changes in NEP are controlled by changes in NPP and in RH. In the model, RH is a function of the soil and litter carbon content and of the decomposition rate (equations (2) and (3)). Therefore, climate can affect RH directly through the decomposition rate, but also indirectly through changes in carbon pools size (subsequent to changes in NPP and litterfall).

[32] In the tropics, litter and soil carbon are drastically reduced (Table 2) mainly because of the strong reduction of carbon input. This directly leads to a quasi proportional reduction of RH. The direct climate impact on RH is relatively small: The decomposition rate increase following the warming is partially reduced by a decrease due to the tropical soil drying (Figure 5b).

[33] In the Northern Hemisphere, the small climate induced increase of tundra and conifers NPP does not translate into any increase in litter and soil carbon. The climate induced increase in RH is therefore due to an acceleration of the decomposition rate which follows the large increase of surface temperature. Deciduous forests do not show any increase of NPP, but they show a large increase in decomposition rate which leads to an increase of RH and a decrease in litter and soil carbon (Table 2). Temperate grasslands and croplands have a behavior similar to the one observed in the tropics : a decrease of NPP which drives a decrease in pool size and therefore in RH.

5.2. Analysis of the Mechanism Driving the Climate Induced Changes In Land Carbon Cycle

[34] In this section, we highlight the mechanisms that drive the ecosystems response to climate change. Our terrestrial biospheric model is driven by three external climate variables: surface temperature, precipitation, and incoming solar radiation (Figure 6). To separate the impact of each variable on the terrestrial biosphere, we performed three offline simulations (Table 1, Temperature Impact, Precipitation Impact and Radiation Impact simulations)

where two of the forcing variables are set to their control value and the third one is taken from the Climate Impact run. In those simulations, atmospheric CO_2 is also set equal to the one of the Climate Impact run.

[35] As shown in Figure 6, temperature has a direct control on growth and decomposition rate but also an indirect control on these fluxes through soil water content (equations (1) and (3)). Indeed, soil water content is calculated in SLAVE from a balance between precipitation, evapotranspiration, which directly depends on temperature, and runoff. A decrease in soil water content will tend to reduce NPP and soil decomposition, whereas a large increase in soil water content may also decrease decomposition if soils become water saturated. To separate the overall impact of temperature change on land biospheric fluxes from the one specifically due to change in soil humidity, we ran a fourth simulation where all climate variables are set to their Control value except for the calculation of soil water budget where we used temperature and precipitation from the Climate Impact run (Soil Water Content Impact simulation, Table 1).

5.2.1. Tropics and Southern Hemisphere

[36] In the tropics, we find that future evolution of both temperature and precipitation have a negative impact on tropical NPP, temperature being the main driver for the tropical NPP response to climate change (Table 3). The Temperature Impact and the Soil Water Content Impact simulations show basically the same response for NPP, meaning that the impact of higher temperature is primarily indirect, via the reduction of soil water content. Elevated temperatures lead to an increase in water stress on tropical vegetation (Figure 5b), explaining the reduction of NPP. This effect is common to seasonal and evergreen tropical forests and savannas (Figure 7), where loss of soil water is of 20% by 2100. Over evergreen tropical forests, we simulate a slight increase in precipitation, which is too low to counterbalance the large temperature effect (Table 3). We also find that change in radiation alone has a negligible positive impact on tropical productivity (Table 3).

[37] As mentioned before, the response of RH follows the one of NPP. Overall, the strong NEP reduction we simulate in the tropics is mainly due to the indirect impact of temperature on NPP through a reduction of soil water content.

5.2.2. Middle and High Northern Latitudes

[38] In the Northern Hemisphere middle and high latitudes, for all ecosystems, the direct impact of elevated temperature on NPP is quite important. Tundras and coniferous forests experience a longer growing season with favorable temperature. For these ecosystems, this mechanism explains the overall increase of NPP under climate change (Figure 7). For deciduous forests, temperate grasslands and croplands, the direct effect of temperature on NPP is also present, however, it is counterbalanced by the impact of reduced soil moisture on NPP (Table 3 and Figure 7). This latter is due to the combination of higher surface temperature and reduction of summer precipitation. We also find that the increase of incoming radiation during the summer tends to increase NPP.

[39] Concerning tundras and conifers, the NEP changes follow changes in NPP, that is a slight increase because of

Table 3. Change in NPP Attributable to Increased Atmospheric CO_2, Climate Change and Change in Specific Climate Variable[a]

	Global	Tropics (90°S 30°N)	North (30°N 50°N)	North (50°N 90°N)	Tundras	Conifer Forests	Deciduous Forests (Trop/Temp)	Grasslands (Trop/Temp)	Savannas	Seasonnal Evergreen Tropical Forests	Tropical Forests	Croplands (Trop/Temp)
Fertilization effect	+35.5	+23.6	+11.9	+7.4	+0.5	+3.3	+3.7 (+1.5/+2.2)	+9.10 (+6.4/+2.6)	+3.33	+5.01	+4.12	+5.31 (+2.7/+2.6)
Climate impact	−15.6	−15.3	−0.8	+0.5	+0.18	+0.73	−0.36 (−0.34/−0.01)	−5.70 (−5.2/−0.5)	−2.50	−3.10	−2.30	−1.76 (−1.3/−1.5)
Temperature effect	−12.8	−13.9	+0.5	+0.6	+0.12	+0.80	−0.10 (−0.33/+0.23)	−4.00 (−4.2/+0.2)	−2.24	−2.90	−2.41	−1.38 (−1.2/−0.2)
Precipitation effect	−5.5	−3.0	−2.0	−0.5	+0.02	−0.15	−0.40 (+0.04/−0.44)	−2.60 (−1.6/−1.0)	−0.64	−0.65	+0.30	−0.82 (−0.2/−0.6)
Radiation effect	+2.3	+1.4	+0.6	+0.3	+0.01	+0.15	+0.12 (−0.05/+0.17)	+0.85 (+0.6/+0.3)	+0.31	+0.51	+0.10	+0.38 (+0.1/+0.3)
Soil water content effect	−19.8	−14.5	−4.4	−1	+0.00	−0.55	−1.16 (−0.26/−0.90)	−7.03 (−5.1/−1.9)	−2.50	−3.14	−1.73	−2.73 (−1.2/−1.5)

[a]See Table 1 for more details. Values in parentheses are for tropical regions (30°S–30°N) and for temperate regions (30°N–50°N).

higher temperature. For deciduous forests, where NPP does not increase, the decrease in NEP is explained by an increase of RH as the decomposition rate is favored by warmer temperature. The temperate grasslands and croplands NEP reduction follows the NPP one, as RH is reduced since the litter and soil carbon pool size are decreased.

5.3. Response of the Seasonal Amplitude of Land Biospheric Fluxes to Climate Change

[40] Careful analysis of the seasonal behavior of NEP in our simulation makes it possible to derive additional infor-mation on the respective role of NPP and RH. The evolution of the amplitude of NEP seasonal cycle in mid and high latitude bands of the Northern Hemisphere is represented in Figure 8.

5.3.1. High Northern Latitudes

[41] At high northern latitudes (>50°N) the NEP seasonal peak to peak amplitude in the Climate Impact run increases by 55% in 2100 (Figure 8). This increase is mainly due to rising atmospheric CO_2 (by 52%) stimulat-ing NPP (Figure 9). Temperature change increases NPP and RH amplitudes by direct effect but decreases them by indirect effect via soil water content. Precipitation change
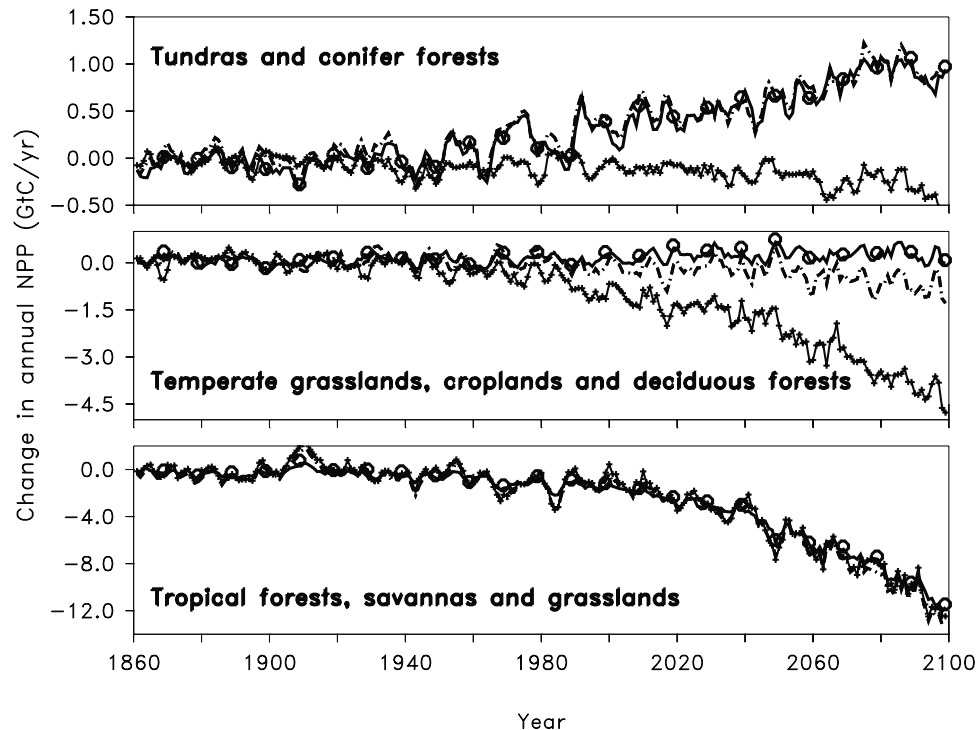

Figure 7. Time series of the impact of change in climate (dash-dotted line), temperature (line of circles), and soil water content (line of crosses) on NPP (Gt C yr^{-1}).
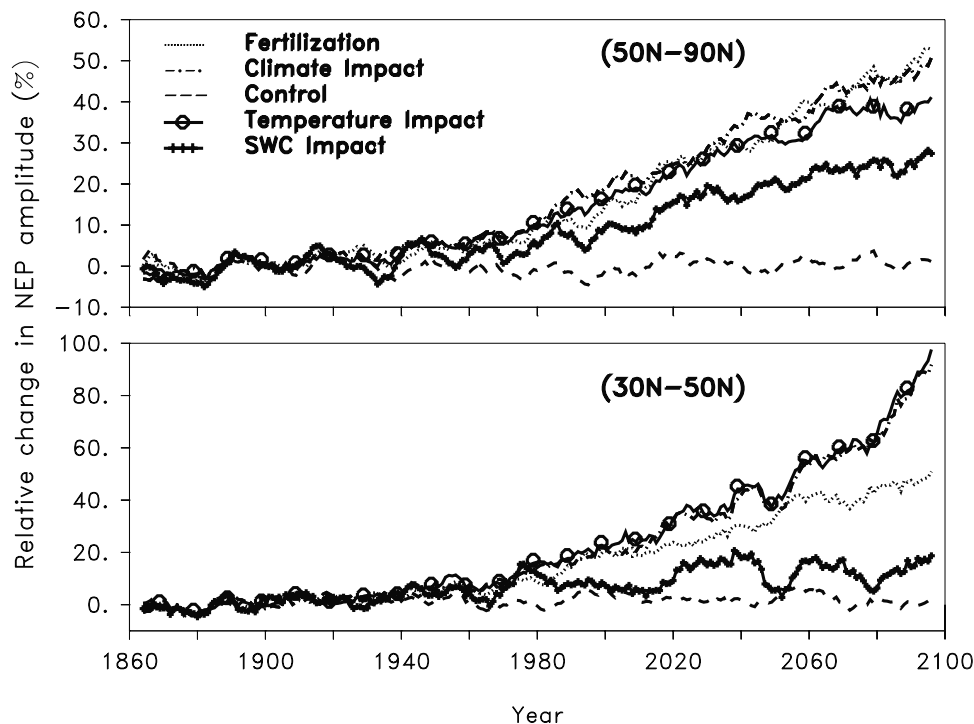
Figure 8. Time series of the evolution of the amplitude of NEP relative to 1860 for the 50°N–90°N latitudinal band and for the 30°N–50°N latitudinal band for the Control simulation (dashed line), the Fertilization simulation (dotted line), the Climate Impact simulation (dash-dotted line), the Temperature Impact simulation (line of circles), and the Soil Water Content Impact simulation (line of crosses).

which increases soil water content leads to a small amplitude increase. Overall, climate change has a negligible impact on the change of amplitude of NEP as both the NPP and RH amplitude are affected the same way by climate.

5.3.2. Middle Northern Latitudes

[42] The model results in the mid northern latitudes are drastically different from the high latitudes (Figure 8). Between 30°N and 50°N, the increase in NEP amplitude of the Climate Impact run is greater than north of 50°N and reaches 95% by 2100. The fertilization effect and the effect of temperature change on NEP amplitude are of the same order, 50% of this increase is due to the increase of atmospheric CO_2 and 45% is due to temperature change. This climate induced increase in NEP amplitude mainly occurs in the late summer as the terrestrial biosphere becomes a strong source of carbon (Figure 9).

[43] The simulated seasonal amplitude of NPP decreases under climate change (Figure 9). NPP is reduced in summer as a result of two factors: (1) warmer temperature and reduced precipitation which increases water stress on productivity and (2) warmer temperature which directly increases the heat stress on productivity. Indeed, during this period, simulated temperature exceed optimum temperature (18°C) (Figure 10). As a result, the maximum of NPP occurs in May in the Climate Impact run, whereas it occurs in June in the Fertilization run.

[44] RH amplitude is not affected by the climate change. Indeed, it is stimulated by the increasing temperature (especially in spring and summer) but reduced by the reduced soil water content (during the whole year) (Figure 9).

[45] Overall, the large NPP reduction in summer induces a strong NEP source in July and August (Figure 9). This explains the climate induced increase of NEP seasonal cycle amplitude.

5.4. Response of the Growing Season Length to Climate Change

[46] We define the length of the growing season net flux as the period where NPP exceeds RH.

5.4.1. High Northern Latitudes

[47] Figure 11 represents the evolution of the onset and the offset of the growing season for the high latitudes (>50°N). Though the increasing atmospheric CO_2 has shown an impact on NEP seasonal amplitude, it shows no impact on the duration of the growing season (comparison between Fertilization and Control runs). The simulated growing season is lengthened by about 18 days by 2100, because of an earlier onset (12 days) and of a later termination (6 days).

[48] The earlier onset is essentially due to changes in temperature. As mentioned in the previous section, the maximum of NPP and hence NEP occurs earlier in the year as spring temperature are closer to the optimum temperature in the Climate Impact run (Figure 10). The end of the growing season is controlled by two opposite phenomena: It is delayed by about 7.5 days because of warmer temper-
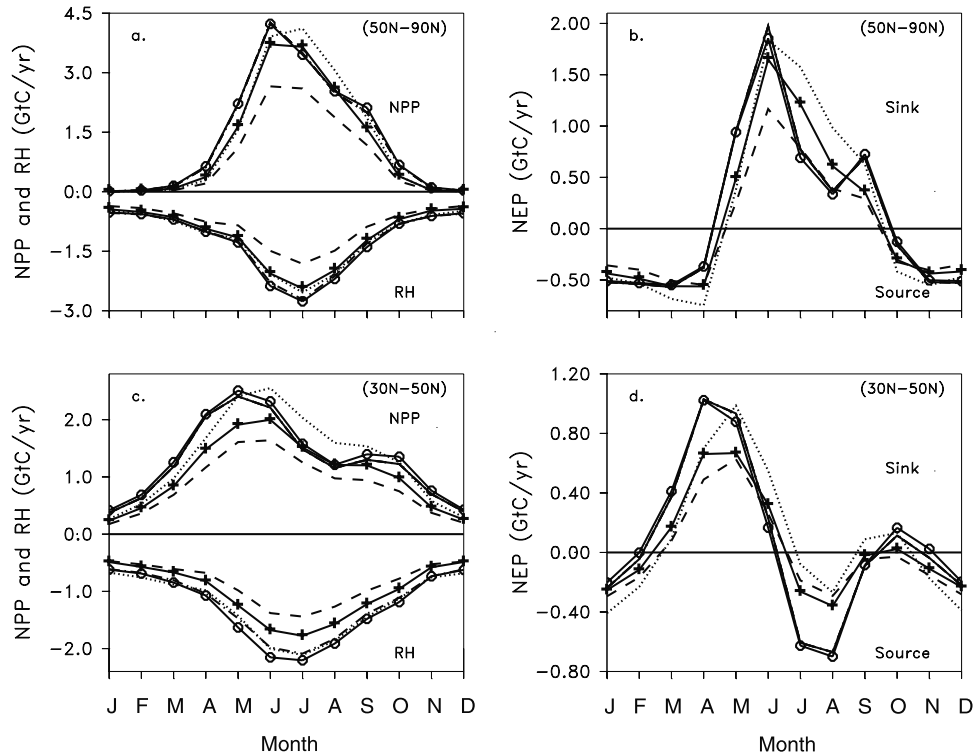
Figure 9. Mean seasonal cycle averaged over the last 20 years of the simulation (2080–2100) of (a) NPP and RH for the Control simulation (dashed line), the Fertilization simulation (dotted line), the Climate Impact simulation (dash-dotted line), the Temperature Impact simulation (line of circles), the Soil Water Content Impact simulation (line of crosses) for the 50°N–90°N latitudinal band, (b) same as Figure 9a for NEP, (c) same as Figure 9a for the 30°N–50°N latitudinal band, and (d) same as Figure 9b for the 30°N–50°N latitudinal band.

atures but it is advanced by about 1.5 days because of lower soil water content (Figure 10).

5.4.2.   Middle Northern Latitudes

[49] In 30°N–50°N, the growing season net flux is more difficult to evaluate because of the shape of the NEP signal. We simulate a net carbon uptake from March to June and a release from July to September, then a net carbon uptake between October and November and finally a release from December to February (Figure 11). The beginning of the growing season is advanced by 15 days. It can be explained by the same reason than for the high latitudes: direct impact of higher temperatures on spring NPP. Because of the particular shape of NEP in late summer and fall, we cannot estimate any change in the offset of the growing season.

6.   Discussion and Conclusions

[50] To understand the role of the terrestrial biosphere in controlling future atmospheric CO_2 and indirectly future climate change, we analyzed several simulations from a coupled climate-carbon model forced by an SRES-A2 IPCC scenario of fossil fuel and deforestation CO_2 emissions [*Dufresne et al.*, 2002].

[51] For the coming century, the simulated increase of terrestrial uptake due to higher atmospheric CO_2 is partially reduced because of climate change (difference of 228 Gt C between the Fertilization and the Climate Impact simula-

tions). The global land biospheric response is largely driven by the tropical ecosystems (decrease in storage by 215 Gt C), which are strongly affected by drought stress. After 2050, some regions in the tropics even become sources of carbon. Only at high latitudes of the Northern Hemisphere, our model predicts that photosynthesis will, on the contrary, be stimulated by the increase of surface temperature which extends the growing season of the terrestrial biosphere.

[52] The global reduction of carbon uptake induces an increase of atmospheric CO_2 (78 ppmv by 2100) which in turn enhances the terrestrial uptake. Overall, this "additional" fertilization effect slightly reduces the negative impact of climate on the terrestrial storage. The climate change alone induces a global reduction of 228 Gt C while the additional CO_2 leads to an extra storage of 53 Gt C.

[53] However, the result described above are very likely to be climate and carbon models dependent. Indeed, the OAGCMs vary considerably in their ability to simulate climate change. Previous climate change OAGCMs intercomparison studies [*IPCC*, 2001; *Meehl et al.*, 2000; *Räisänen*, 2001] have shown that the OAGCMs agreement to simulate temperature change is very good in most of the world whereas there is very little agreement in the simulation of precipitation change (especially in tropics). As tropics are the regions where we simulate the largest carbon uptake reduction, we can expect our results to be somehow dependent on the OAGCM used. However, the Hadley
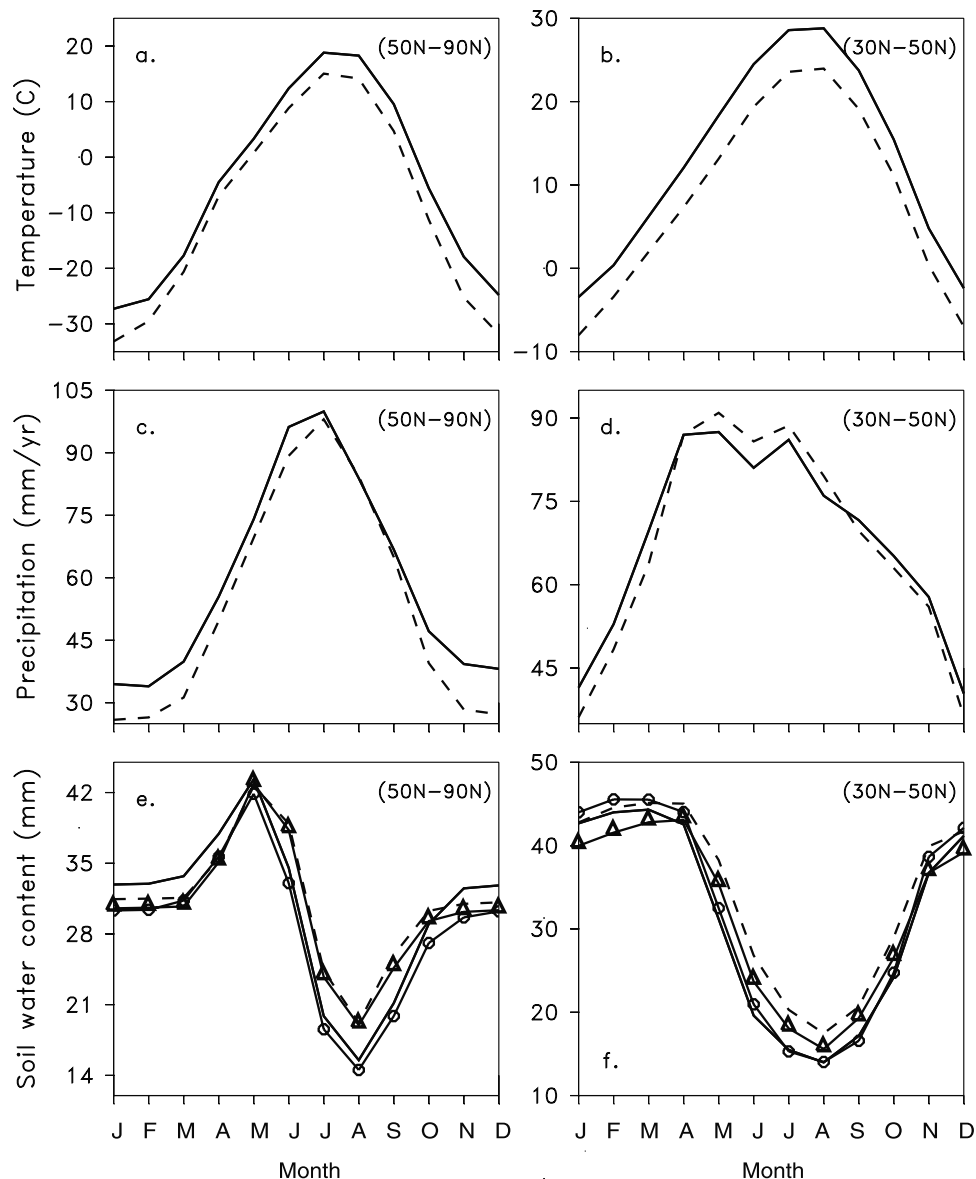
Figure 10. Mean seasonal cycle averaged over the last 20 years of the simulation (2080–2100) of (a) temperature for the Control simulation (dashed line), and the Coupled Scenario simulation (solid line) for the 50°N–90°N latitudinal band, (b) same as Figure 10a for the 30°N–50°N latitudinal band, (c) same as Figure 10a for precipitation and (d) same as Figure 10b for precipitation. (e) Same as Figure 10a for soil water content with the Temperature Impact simulation (line of circles) and the Precipitation Impact simulation (line of triangles) and (f) same as Figure 10e for the 30°N–50°N latitudinal band.

OAGCM that has been used in the same context shows results consistent with ours: a reduction of tropical NEP because of climate change [*Cox et al.*, 2000].

[54] As we use different climate and carbon cycle models in this study, the uncertainty in the results can come from both sides. To evaluate roughly the consequences of the way we model the climate-carbon cycle system, we compare the results of our study to the *Cox et al.* [2000] coupled simulation.

[55] *Cox et al.* [2000] used the Hadley model to investigate the climate-carbon cycle feedback. By 2100, atmospheric CO_2 reaches 980 ppmv in the Hadley coupled simulation, whereas it only amounts to 770 ppmv in our coupled simulation. Reasons for such a large difference are mainly due to the land biosphere response to climate change. The IPSL cumulated terrestrial net storage amounts to 465 Gt C in 2100 whereas the Hadley model simulates a net source to the atmosphere of 100 Gt C.

[56] In the IPSL simulation, the terrestrial biosphere does not become a global source of carbon. We only locally simulate net carbon release to the atmosphere (in South America) due to the soil drying which induces a saturation of NPP. Several differences between the IPSL and Hadley simulations require further attention. First, the IPSL parti-
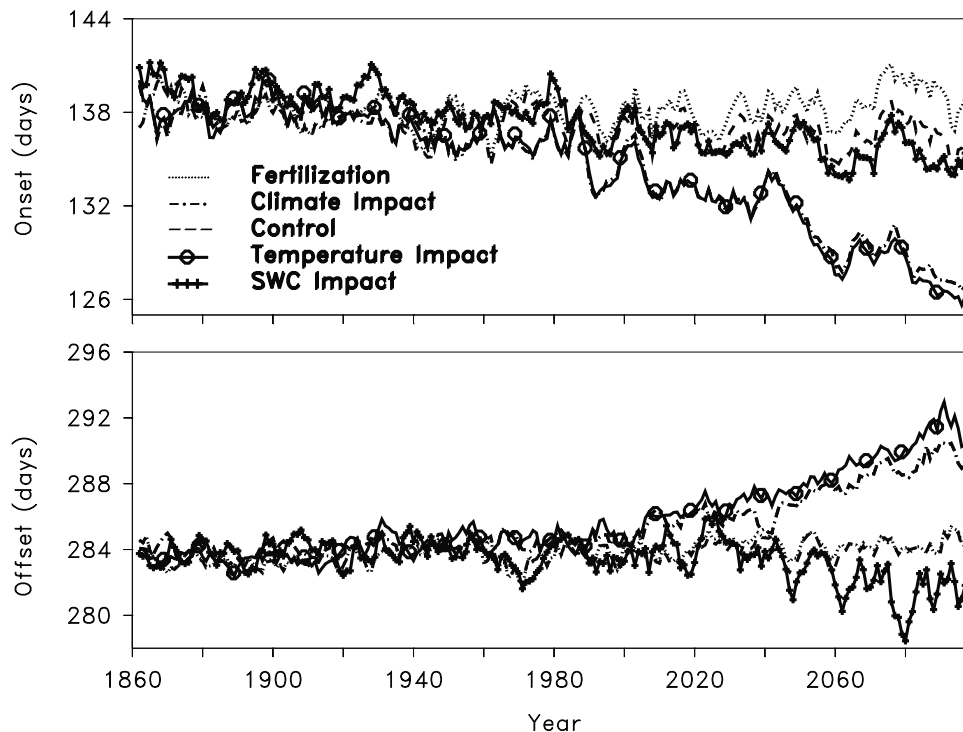
Figure 11. Time series of the evolution of the onset and of the offset of NEP growing season for the 50°N–90°N latitudinal band for the Control simulation (dashed line), the Fertilization simulation (dotted line), the Climate Impact simulation (dash-dotted line), the Temperature Impact simulation (line of circles) and the Soil Water Content Impact simulation (line of crosses).

tioning of excess carbon due to the increase of atmospheric CO_2, without climate change, is greater in the vegetation (400 Gt C in 2100) than in soils (200 Gt C) whereas Hadley terrestrial biosphere has the opposite behavior. The partitioning of carbon in above versus below ground pools in the IPSL coupled simulation is similar to the one of previous simulations conducted offline [*Cramer et al.*, 2001]. Whether the excess carbon will, in the future, go preferentially in the vegetation or in the soil is still an open question. Second, the impact of climate change on soils is much larger in the Hadley simulation (reduction of 550 Gt C in 2100) than in the IPSL one (reduction of 100 Gt C) or in the various land biosphere models analyzed by *Cramer et al.* [2001] (reduction of 150 Gt C averaged across models). This could partly be due to the large storage in the Hadley soil model under increased CO_2 only. We also found in our simulations that soil respiration generally decreases because NPP and hence soil carbon input decreases under climate change, a mechanism not seen in the Hadley simulations. This may be due to different assumptions in soil turnover times in the two models. Third, another difference between the Hadley framework and ours is the inclusion of a dynamic vegetation model in Hadley model: drought stress initiates loss of Amazonian forest, which also contribute to release carbon to the atmosphere. In the IPSL simulation, the land biosphere model uses a fixed distribution of ecosystems, thus neglecting the impact of climate on the vegetation distribution and also neglecting the importance that such processes may have in the future, for example by reducing plants population or NPP [*Cox et al.*, 2000;

Cramer et al., 2001]. As explained in section 2.2, we decided not to account for future scenario of land use and therefore we preferred not to account for vegetation dynamic at all. It is worth noting that both simulations suffer from severe simplifications.

[57] Regarding the modeling of climate change, we do not account for changes in aerosols emissions that are very likely to come along with CO_2 emissions. Atmospheric chemistry as a whole is not accounted for in such simulations. Future works should consider the evolution of aerosols and other greenhouse gases in the atmosphere and their control on the Earth radiative budget [*Haywood and Boucher*, 2000; *Jacobson*, 2001].

[58] Regarding the carbon cycle, we manage to simulate annual atmospheric CO_2 from 1860 to 2000, however, we do not include some terrestrial processes that are very likely to play an important role in the net land uptake. Indeed, we assume that the uptake is only driven by climate and atmospheric CO_2, whereas anthropogenic nitrogen deposition and land cover changes are also believed to play a large role. Several studies estimated the importance of anthropogenic nitrogen deposition on terrestrial carbon cycle [*Holland et al.*, 1997; *Nadelhoffer et al.*, 1999]. The role played by anthropogenic nitrogen remains largely uncertain but could be significant and should be included in future climate-carbon cycle studies. Another potentially large component of the present-day terrestrial uptake is due to forest regrowth in the temperate regions *Caspersen et al.*, 2000; *Joos et al.*, 2002; *Pacala et al.*, 2001; *Schimel et al.*, 2001. Such processes are also not included in the present

climate-carbon simulations. Future simulations, should clearly use historical land cover changes data and future land cover changes scenarios.

[59] In summary, even without considering all the processes that can affect land carbon cycle, our results highlight the crucial role that the land biosphere may play in future climate change. Despite large sources of uncertainties, it is generally found that land biospheric carbon pools may be affected by the climate change leading to a positive feedback between carbon cycle and climate system. However, its amplitude is still uncertain. Intercomparison project of climate-carbon cycle models should help to better understand the mechanisms involved in the feedback [*Cox et al.*, 2002].

[60] It is also clear that such experiments are still very idealized, rather than credible simulations of what will happen in the future. Even if the results of this study are roughly consistent with observations during the historical period, it is likely that not considering all involved processes may lead to uncertainties and that improving terrestrial carbon cycle models is of the uppermost importance, just like improving GCM predictions.

References

Andres, R., G. Marland, I. Fung, and E. Matthews, A $1° \times 1°$ of carbon dioxide emissions from fossil fuel consumption and cement manufacture, 1950–1990, *Global Biogeochem. Cycles*, 10, 419–429, 1996.

Aumont, O., Etude du cycle naturel du carbone dans un modèle 3D de l'océan mondial, Ph.D. thesis, Université Pierre et Marie Curie, Paris, 1998.

Bergh, J., S. Linder, T. Lundmark, and B. Elfving, The effect of water and nutrient availability on the productivity of Norway spruce in northern and southern Sweden, *For. Ecol. Manage.*, 119, 51–62, 1999.

Betts, R. A., P. M. Cox, E. L. Susan, and F. I. Woodward, Contrasting physiological and structural vegetation feedbacks in climate change simulations, *Nature*, 387, 796–799, 1997.

Bopp, L., P. Monfray, O. Aumont, J. L. Dufresne, H. L. Treut, G. Made, L. Terray, and J. C. Or, Potential impact of climate change on marine export production, *Global Biogeochem. Cycles*, 15, 81–99, 2001.

Bryant, D. M., E. A. Holland, T. R. Seastedt, and M. D. Walker, Analysis of litter decomposition in an alpine tundra, *Can. J. Bot.*, 76, 1998.

Cao, M., and F. I. Woodward, Dynamic responses of terrestrial ecosystem carbon cycling to global climate change, *Nature*, 393, 249–252, 1998.

Caspersen, J. P., S. W. Pacala, J. C. Jenkins, G. C. Hurtt, P. R. Moorcroft, and R. A. Birdsey, Contributions of land-use history to carbon accumulation in US forests, *Science*, 290, 1148–1151, 2000.

Cox, P. M., R. A. Betts, C. D. Jones, A. S. Spal, and I. J. Totterdell, Acceleration of global warming due to carbon-cycle feedbacks in a coupled climate model, *Nature*, 408, 184–187, 2000.

Cox, P., P. Friedlingstein, and P. Rayner, Modelling climate-carbon cycle feedbacks: A cross disciplinary collaboration priority, *Global Change News Lett.*, 49, 12–14, 2002.

Cramer, W., et al., Global response of terrestrial ecosystem structure and function to CO2 and climate change: Results from six dynamic global vegetation models, *Global Change Biol.*, 7, 357–373, 2001.

Cubasch, U., and I. Fisher-Bruns, An intercomparison of scenario simulations performed with different AOGCMs, 4, report, Norw. Meteorol. Inst., Blindern, Norway, 2000.

Delecluse, P., G. Madec, M. Imbard, and C. Lévy, OPA version 7, Ocean General Circulation Model Reference Manual, tech. rep., Inst. Pierre-Simon Laplace, 1993.

DeLucia, E. H., et al., Net primary production of a forest ecosystem with experimental CO2 enrichment, *Science*, 284, 1177–1179, 1999.

Dufresne, J. L., P. Friedlingstein, M. Berthelot, L. Bopp, P. Ciais, L. Fairhead, and P. Monfray, On the magnitude of positive feedback between future climate change and the carbon cycle, *Geophys. Res. Lett.*, 29, 1405, doi:10.1029/2001GL013777, 2002.

Etheridge, D., L. Steele, R. L. Langenfelds, R. J. Francey, J. M. Barnola, and V. I. Morgan, Natural and anthropogenic changes in atmospheric CO2 over the last 1000 years from air in Antarctic ice and firn, *J. Geophys. Res.*, 101, 4115–4128, 1996.

Friedli, H., H. Lötscher, H. Oeschger, U. Siegenthaler, and B. Stauffer, Ice core record of the 13C/12C ratio of atmospheric CO2 in the past two centuries, *Nature*, 324, 237–238, 1986.

Friedlingstein, P., I. Fung, E. Holland, J. John, G. Brasseur, D. Erickson, and D. Schimel, On the contribution of CO2 fertilization to the missing biospheric sink, *Global Biogeochem. Cycles*, 9, 541–556, 1995.

Friedlingstein, P., L. Bopp, P. Ciais, J. L. Dufresne, L. Fairhead, H. LeTreut, P. Monfray, and J. C. Orr, Positive feedback between future climate change and the carbon cycle, *Geophys. Res. Lett.*, 28, 1543–1546, 2001.

Haywood, J., and O. Boucher, Estimates of the direct and indirect radiative forcing due to tropospheric aerosols: A review, *Rev. Geophys.*, 38, 513–543, 2000.

Holland, E. A., B. H. Braswell, J. F. Lamarque, A. Townsend, J. Sulzman, J. F. Müller, F. Dentener, G. Brasseur, H. L. III, J. E. Penner, and G. J. Roelofs, Variations in the predicted spatial distribution of atmospheric nitrogen deposition and their impact on carbon uptake by terrestrial ecosystems, *J. Geophys. Res.*, 102, 15,849–15,866, 1997.

Intergovernmental Panel on Climate Change, *Climate Change 2001: The Scientific Basis - Contribution of Working Group I to the IPCC Third Assessment Report*, Cambridge Univ. Press, New York, 2001.

Jacobson, M. Z., Strong radiative heating due to the mixing state of black carbon in atmospheric aerosols, *Nature*, 409, 695–697, 2001.

Joos, F., I. C. Prentice, and J. I. House, Growth enhancement due to global atmospheric change as predicted by terrestrial ecosystem models: Consistent with U.S. forest inventory data, *Global Change Biol.*, 8, 299–303, 2002.

Kawamura, K., T. Nakazawa, T. Machida, S. Morimoto, S. Aoki, Y. Fujii, and O. Watanabe, Precise estimates of the atmospheric CO2 concentration and its carbon isotopic ratio during the last 250 years from an Antarctic ice core, H15, paper presented at 5th International Carbon Dioxide Conference, Commonw. Sci. and Ind. Res. Org., Cairns, Australia, 1997.

Keeling, C. D., T. P. Whorf, M. Wahlen, and J. vanderPlicht, Interannual extremes in the rate of rise of atmospheric carbon dioxide since, *Nature*, 375, 666–670, 1995.

Keeling, C. D., J. F. S. Chin, and T. P. Whorf, Increased activity of northern vegetation inferred from atmospheric CO2 measurements, *Nature*, 382, 146–149, 1996.

Keyser, A. R., J. S. Kimball, R. R. Nemani, and S. W. Running, Simulating the effects of climate change on the carbon balance of north American high-latitude forests, *Global Change Biol.*, 6, 185–195, 2000.

King, A. W., W. M. Post, and S. D. Wullschleger, The potential response of terrestrial carbon storage to changes in climate and atmospheric CO2, *Clim. Change*, 35, 199–227, 1997.

LeTreut, H., and Z. X. Li, Sensitivity of an Atmospheric General Circulation Model to prescribed SST changes: Feedback effects associated with the simulation of cloud optical properties, *Clim. Dyn.*, 5, 175–187, 1991.

Lloyd, J., The CO2 dependence of photosynthesis, plant growth responses to elevated CO2 concentrations and their interaction with soil nutrient status, II, Temperate and boreal forest productivity and the combined effects of increasing CO2 concentrations and increased nitrogen deposition at a global scale, *Funct. Ecol.*, 13, 439–459, 1999.

Maier-Reimer, E., Geochemical cycles in an ocean general circulation model: Preindustrial tracer distributions, *Global Biogeochem. Cycles*, 7, 645–677, 1993.

Matthews, E., Global vegetation and land use: New high resolution data bases for climate studies, *J. Clim. Appl. Meteorol.*, 22, 474–487, 1983.

McGuire, A. D., et al., Carbon balance of the terrestrial biosphere in the twentieth century: Analyses of CO2, climate, and land use effects with four process-based ecosystem models, *Global Biogeochem. Cycles*, 15, 183–206, 2001.

Meehl, G. A., G. J. Boer, C. Covey, M. Latif, and R. J. Stouffer, The Coupled Model Intercomparison Project (CMIP), *Bull. Am. Meteorol. Soc.*, 81, 313–318, 2000.

Melillo, J. M., A. D. McGuire, D. W. Kicklighter, B. Moore, C. J. Vorosmarty, and A. L. Schloss, Global climate change and terrestrial net primary production, *Nature*, 363, 234–240, 1993.

Menzel, A., and P. Fabian, Growing season extended in Europe, *Nature*, 397, 659, 1999.

Myneni, R. B., C. D. Keeling, C. J. Tucker, G. Asrar, and R. R. Nemani, Increased plant growth in the northern high latitudes from 1981 to 1991, *Nature*, 386, 698–702, 1997.

Nadelhoffer, K. J., B. A. Emmett, P. Gundersen, O. J. Kjonaas, C. J. Koopmans, P. Schleppi, A. Tietema, and R. F. Wright, Nitrogen deposition makes a minor contribution to carbon sequestration in temperate forests, *Nature*, *398*, 145–148, 1999.

Nakicenovic, N., et al., IPCC special report on emissions scenarios, report, Intergov. Panel on Clim. Change, New York, 2000.

Neilson, R. P., and R. J. Drapek, Potentially complex biosphere responses to transient global warming, *Global Change Biol.*, *4*, 505–521, 1998.

Pacala, S. W., et al., Consistent land- and atmosphere-based US carbon sink estimates, *Science*, *292*, 2316–2320, 2001.

Parton, W. J., et al., Observations and modeling of biomass and soil organic matter dynamics for the grassland biome worldwide, *Global Biogeochem. Cycles*, *7*, 785–809, 1993.

Potter, C. S., J. T. Randerson, C. B. Field, P. A. Matson, P. M. Vitousek, H. A. Mooney, and S. A. Klooster, Terrestrial ecosystem production: A process model based on global satellite and surface data, *Global Biogeochem. Cycles*, *7*, 811–841, 1993.

Räisänen, J., CO_2 induced climate change in CMIP experiments: Quantification of agreement and role of internal variability, *J. Clim.*, *14*, 2088–2104, 2001.

Randerson, J. T., C. B. Field, I. Y. Fung, and P. P. Tans, Increases in early season ecosystem uptake explain recent changes in the seasonal cycle of atmospheric CO_2 at northern latitudes, *Geophys. Res. Lett.*, *26*, 2765–2768, 1999.

Saugier, B., and J. Roy, Estimations of global terrestrial productivity: Converging towards a single number?, in *Global Terrestrial Productivity: Past, Present and Future*, edited by J. Roy, B. Saugier, and H. A. Mooney, pp. 541–555, Academic, San Diego, Calif., 2001.

Schimel, D. S., et al., Recent patterns and mechanisms of carbon exchange by terrestrial ecosystems, *Nature*, *414*, 169–172, 2001.

Sellers, P. J., D. A. Randall, G. J. Collatz, J. A. Berry, C. B. Field, D. A. Dazlich, C. Zhang, G. D. Collelo, and L. Bounoua, A revised land-surface parameterization (Sib2) for atmospheric GCMs I, Model formulation, *J. Clim.*, *9*, 676–705, 1996.

Terray, l., E. Sevault, E. Guilyardi, and O. Thual, The OASIS Coupler User Guide Version 2.0, *Tech. Rep.TR/CMGC/95-46*, Eur. Cent. for Res. and Adv. Training in Sci.Comput. (CERFACS), Toulouse, France, 1995.

Thornthwaite, C. W., An approach toward a rational classification of climate, *Geogr. Rev.*, *38*, 55–89, 1948.

Thornthwaite, C. W., and J. R. Mather, Instructions and tables for computing potential evapotranspiration and the water balance, *Publ. Climatol.*, *10*, 181–311, 1957.

Townsend, A. R., B. H. Braswell, E. A. Holland, and J. E. Penner, Spatial and temporal patterns in terrestrial carbon storage due to deposition of fossil fuel nitrogen, *Ecol. Appl.*, *6*, 806–814, 1996.

Wullschleger, S. D., W. M. Post, and A. W. King, On the potential for a CO_2 fertilization effect in forests: Estimates of the biotic growth factor based on 58 controlled-exposure studies, in *Biotic Feedbacks in The Global Climatic System: Will the Warming Feed the Warming?*, edited by G. M. Woodwell and F. T. Mackenzie, pp. 85–107, Oxford Univ. Press, New York, 1995.

Zimov, S. A., S. P. Davidov, G. M. Zimova, A. I. Davidova, F. S. Chapin III, M. C. Chapin, and J. F. Reynolds, Contribution of disturbance to increasing seasonal amplitude of atmospheric CO_2, *Science*, *284*, 1973–1976, 1999.

———————————

M. Berthelot, P. Ciais, P. Friedlingstein, and P. Monfray, Institut Pierre-Simon Laplace, Laboratoire des Sciences du Climat et de l'Environnement, CEA - Saclay, L'Orme des Merisiers, 91191 Gif sur Yvette, France. (mberthe@lsce.saclay.cea.fr; ciais@lsce.saclay.cea.fr; pierre@lsce.saclay.cea.fr; monfray@lsce.saclay.cea.fr)

J. L. Dufresne, L. Fairhead, and H. Le Treut, Institut Pierre-Simon Laplace, Laboratoire de Météorologie Dynamique, Université Pierre et Marie Curie, 4 place Jussieu, 75252 Paris, France. (Jean-Louis.Dufresne@lmd.jussieu.fr; Laurent.Fairhead@lmd.jussieu.fr; Herve.Letreut@lmd.jussieu.fr)
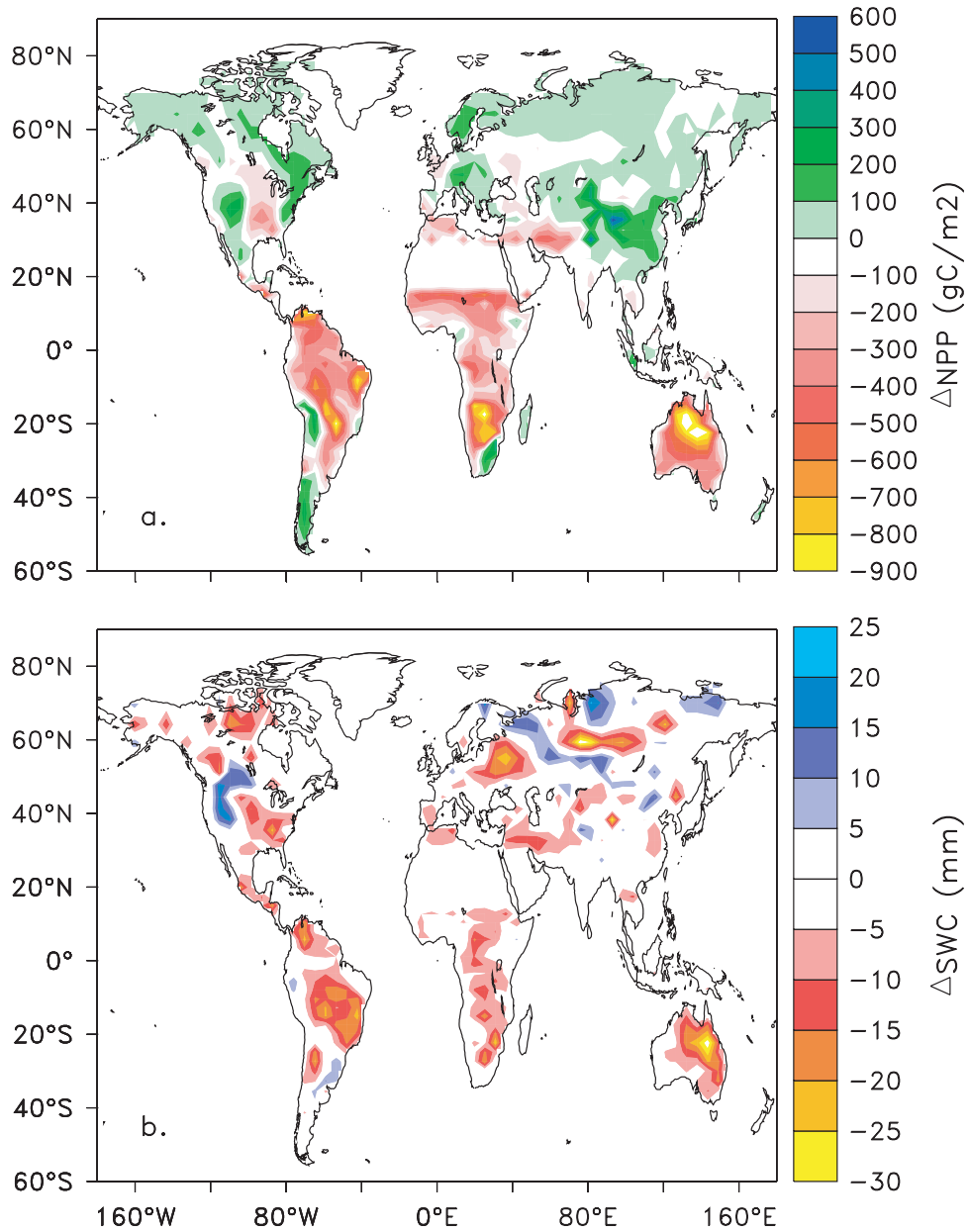
Figure 5. (a) Difference in NPP (in g C/m^2) between the Climate Impact simulation and the Fertilization simulation in 2100 (10-year average). Positive value means that NPP is increased under climate change only. (b) Difference in soil water content (in mm/yr) between the Climate Impact simulation and the Fertilization simulation in 2100 (10-year average). Positive value means that soil water content is increased under climate change.